Supporting Information

On the physicochemical properties, setting chemical reaction, and *in vitro* bioactivity of aragonite-chitosan composite cement as bone substitute

E. Toufik[a,b,c], H. Noukrati[d], C. Rey[c], O. Marsan[c], C. Charvillat[c], S. Cazalbou[e], H. Ben youcef[a] , A. Barroug[b,d*] , C. Combes[c*]

[a]Mohammed VI Polytechnic University (UM6P), HTMR-Lab, 43150 Benguerir, Morocco
[b]Cadi Ayyad University, Faculty of Sciences Semlalia, SCIMATOP-PIB, 40000 Marrakech, Morocco
[c]CIRIMAT, Université de Toulouse, CNRS, Toulouse INP - ENSIACET, 31030 Toulouse, France
[d]Mohammed VI Polytechnic University (UM6P), ISSB-P, 43150 Benguerir, Morocco
[e]CIRIMAT, Université de Toulouse, CNRS, Université Toulouse 3 - Paul Sabatier, 31062 Toulouse, France

**Corresponding author at: CIRIMAT, ENSIACET, 4 allée EmileMonso, 31030 Toulouse Cedex 4, France.*
E-mail address: christele.combes@ensiacet.fr (C. Combes).

**Corresponding author at: Cadi Ayyad University, Faculty of Sciences Semlalia, SCIMATOP-PIB, BP 2390, 40000 Marrakech, Morocco. E-mail address: a.barroug@uca.ac.ma (A. Barroug).*

submitted to *New Journal of Chemistry*

A - Supplementary Note on PONCKS method

To determine the amount of ACC phase, the PONCKS method was applied using the TOPAS software. After carefully determining the continuous background of a pure ACC XRD diagram with a four-order polynomial function, the amorphous envelope of the ACC was modelled with the peaks of an "hkl phase" using a P4 space group with small crystallite size (e.g., 3.5 nm) and unit cell dimensions a = 1 Å and c = 70 Å which were refined. After, the XRD pattern of a 1:1 prepared mixture of ACC:vaterite was inputted in the software. The lattice parameters, crystallite size and relative intensities of the "hkl phase" of the ACC was fixed and the crystal structure of the vaterite was imported[26]. A new refinement was made, for which the continuous background, the lattice parameters, microstrains, crystallite size and scale factor of the vaterite were refined according to the following general equation:

$$W_\alpha = \frac{S_\alpha (ZM \times V)_\alpha}{\sum_{k=1}^{n} S_k \, (ZM \times V)_k}$$

Where k is the number of phases (in our system k = 2, vaterite and ACC), W is the weight fraction or wt% of a phase (for example α), S the Rietveld scale factor of a phase, Z the number of formula units in the unit cell of a phase, M the molecular mass of the formula unit and, V the unit cell volume of a phase.

Thus, for our system, we can write:

$$(ZM)_{ACC} = \frac{W_{ACC}}{W_{vaterite}} \times \frac{S_{vaterite}}{S_{ACC}} \times \frac{(ZM)_{vaterite} \times V_{vaterite}}{V_{ACC}}$$

The calculated $(ZM)_{ACC}$ calibration constant was then entered as cell mass in the "hkl phase" corresponding to the amorphous phase in the TOPAS software. Subsequently, this makes it possible to have directly the mass proportion of ACC at the end of the refinement on a XRD pattern where just the continuous background, the lattice parameters of the crystalline phases, their size of crystallites and microstrains will be refined, as well as the scale factors of all the phases. The method was checked by the analysis of three known mixtures: ACC:vaterite = 0:1, ACC:vaterite = 2:1 and calcite: vaterite: aragonite: ACC = 1:1:1:1. The results are given with an error of ± 2 wt%.

XRD analysis of the synthesised aragonite

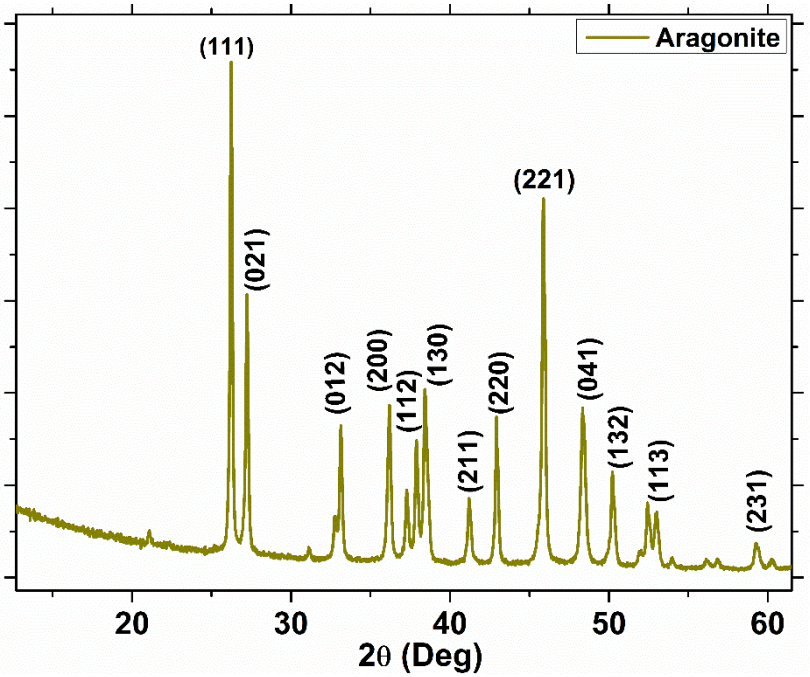

Figure S1: XRD pattern of the synthesised aragonite powder

Lattice parameters of calcite and aragonite in the cements

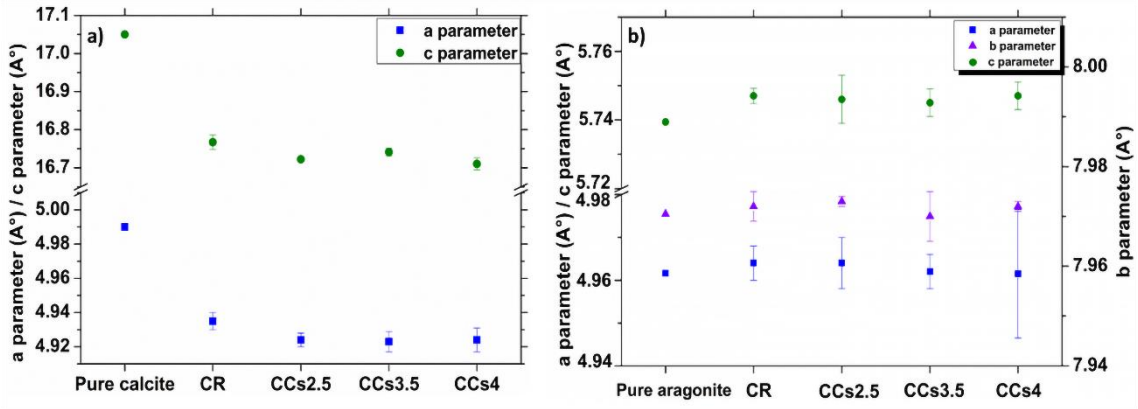

Figure S2: Lattice parameters of a) calcite and b) aragonite formed within the elaborated cement after 48 h of maturation: reference cement (CR), and the composite cements CCs2.5, CCs3.5 and CCs4 prepared with a liquid phase containing 2.5, 3.5 and 4 wt% of chitosan. The calcite within the elaborated cements exhibited smaller lattice parameters with respect to the pure calcite evidencing the incorporation of magnesium within its lattice. The lattice parameters of aragonite within the cements did not change significantly with respect to pure aragonite lattice parameters showing that no significant incorporation

of magnesium occurred.

Raman mapping of composite cement CCs2.5

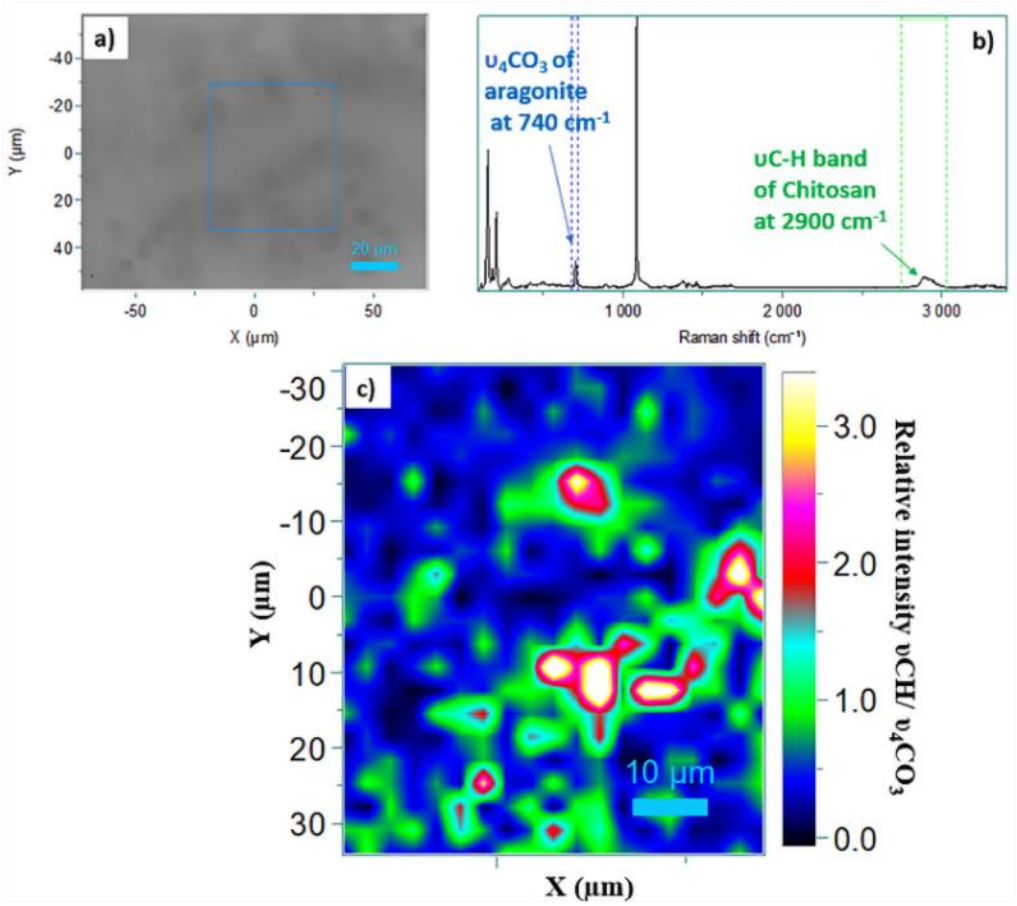

Figure S3: Raman micro-spectroscopic analysis of the hardened composite cement CCs2.5: a) Digital photo of the composite cement surface (after 48 h of maturation time), the blue square indicates the mapped zone, b) Raman spectrum showing the two bands selected for quantitative analysis (νC-H/ν_4CO_3 band surface ratio): at 740 cm^{-1} for aragonite (ν_4CO_3) and at 2900 cm^{-1} for chitosan (νC-H) and, c) Raman mapping based on the νC-H/ν_4CO_3 band surface ratio of the composite cement showing chitosan rich zones.

Setting follow up of the cements using FTIR spectroscopy

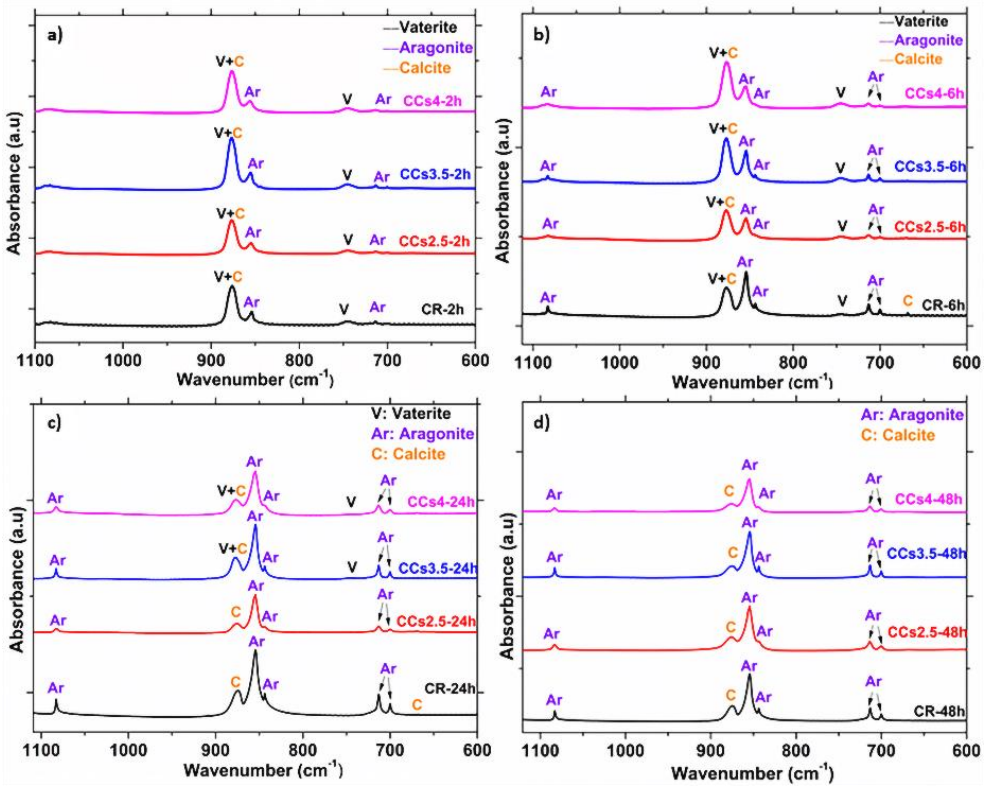

Figure S4: Reference and composite cements composition follow-up using FTIR spectroscopy after a) 2 h, b) 6 h, c) 24 h, and d) 48 h of cement paste maturation at 37°C in a wet atmosphere.

FTIR-ATR analysis of the reactive powders and cements after 2 h of maturation

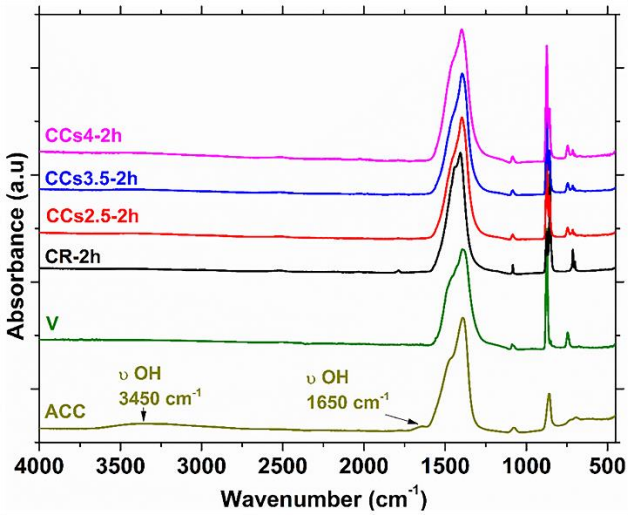

Figure S5: FTIR-ATR spectra of the synthesised reactive powders and cements at 2 h of maturation: ACC is characterised by its unique structural water bands at 1650 cm^{-1} and 3450 cm^{-1}, not observed for the cements at 2 h supporting the absence of unreacted ACC.

Water content determination of ACC using TGA

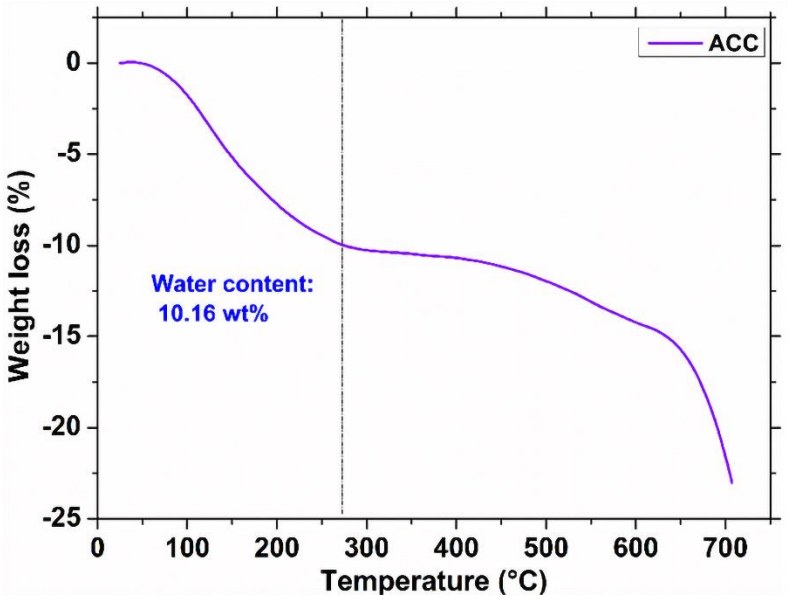

Figure S6: TGA curve of the synthesised ACC.

Chitosan gels used in the composite cement formulations

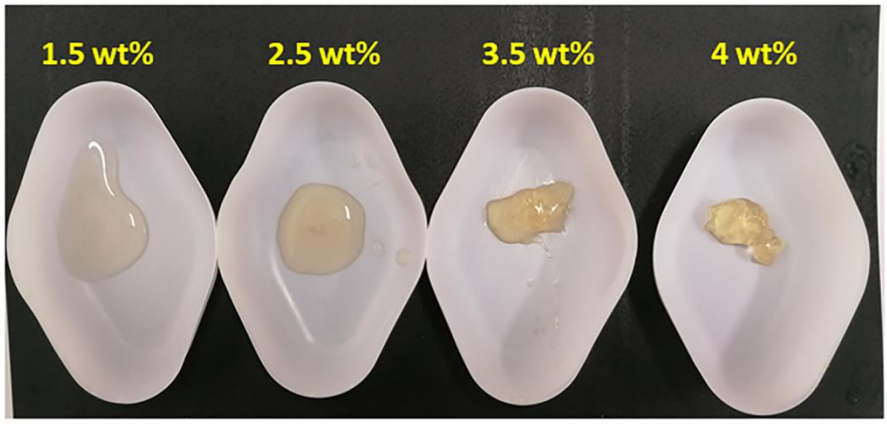

Figure S7: Digital photo of the prepared chitosan hydrogels at different concentrations and used as the liquid phase to prepare the different composite cements.

FTIR spectroscopic analysis of CR and CCs cements after their immersion in SBF

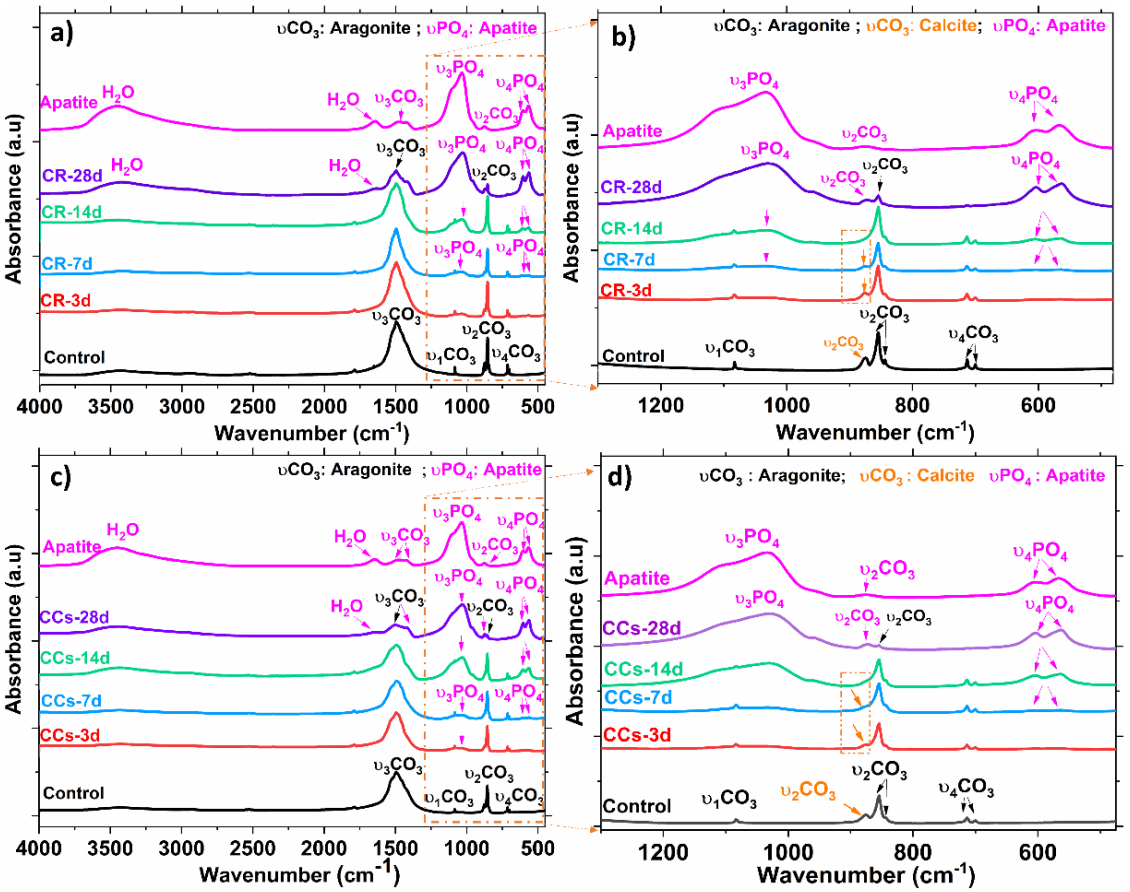

Figure S8: FTIR spectra in function of immersion time in SBF (3 d, 7 d, 14 d, 28 d) of a) CR, b) focus on 500-1300 cm^{-1} domain and c) CCs, d) focus on 500-1300 cm^{-1} domain.

The FTIR spectra show the resorption of calcite within 14 days for both cements evidenced through the disappearance of the calcite υ_2CO_3 band at 875 cm^{-1}. The apatite formation was revealed by the emergence of υ_3PO_4 band at 1031 cm^{-1}, the υ_4PO_4 pair in the 560-590 cm^{-1} range in both cements after 7 days, 14 days and 28 days of immersion time. The apatite formed faster in the composite cement, clearly observed when comparing the relative intensity of the υ_3PO_4 band at 1031 cm^{-1} for both cements after 14 days of immersion in SBF. The υ_2CO_3 band at 872 cm^{-1} shows that the formed apatite is carbonated. The aragonite υ_3CO_3 and υ_2CO_3 bands appeared more intense in CR than in CCs after 28 days of immersion suggesting that apatite formed a thick layer on the surface of CCs which masked aragonite contributions.